9th International Conference on Photonic Technologies - LANE 2016

Laser patterning of CIGS thin films with 1550 nm nanosecond laser pulses

Martin Ehrhardt[a], Pierre Lorenz[a], Lukas Bayer[a], Igor Zagoranskiy[a], Klaus Zimmer[a],*

[a]Leibniz-Institut für Oberflächenmodifizierung e.V., Permoserstraße 15, 04318 Leipzig, Germany

Abstract

The results of laser scribing experiments of CIGS thin films deposited on Mo-coated stainless steel sheets, using laser pulses with a wavelength of 1550 nm and a pulse duration of 6 ns, are presented in this study. It is shown that a removal of the CIGS from the Mo film is possible without edge melting of the CIGS or damaging of the Mo. The critical parameter for inducing the delamination lift-off process of the CIGS from the Mo was identified to be the scribing speed of the laser. In dependence on the laser parameters two different material removal processes were found. For a low pulse overlap the laser pulse penetrates the CIGS film and is absorbed in the interface between the CIGS and the Mo causing a lift-off process of the CIGS from the Mo back contact. For a high pulse overlap an ablation process starting from the top side of the CIGS film was found. The composition and morphology of the sample material after the laser patterning were analysed by scanning electron microscopy (SEM), energy dispersive X-ray spectroscopy (EDX), and micro-Raman spectroscopy.
© 2016 The Authors. Published by Elsevier B.V. This is an open access article under the CC BY-NC-ND license (http://creativecommons.org/licenses/by-nc-nd/4.0/).
Peer-review under responsibility of the Bayerisches Laserzentrum GmbH

Keywords: CIGS; nanosecond, thin film, laser, ablation

1. Introduction

Due to the current developments in the field of electronics, display manufacture and thin-film photovoltaic laser scribing of thermal sensitive thin-film stacks attract significant attention. Especially scribing of thin-film solar cells (TFSC) is of great interest in order to establish this kind of solar modules in the market. Copper indium gallium (di)selenide – $CuIn_xGa_{(1-x)}Se_2$ (CIGS) is one of the most promising material classes for the large-scale production of TFSCs. The theoretically achievable photoelectrical conversion efficiency of $\sim 27\%$ has been predicted for CIGS cells [1]. Experimentally, an efficiency of $\sim 22.3\%$ is reported in Ref. [2] for CIGS material which was deposited on polymer substrates. In order to transfer this high efficiency of CIGS in high-efficient large-area solar cell modules

---

  * Corresponding author. Tel.: +49-341-235-3287 ; fax: +49-(0)341-235-2584 .
    E-mail address: klaus.zimmer@iom-leipzig.de

the CIGS material has to be divided into small segments which are interconnected in series. The serial interconnections of the CIGS material segments allow the reduction of the photocurrent and, in consequence, to reduce the ohmic electrical losses in the module. Mechanical scribing of the CIGS material is limited due to the scribing speed, edge quality, and the distance between two adjacent scribes. To overcome these limitations laser scribing can be performed due to unique characteristics of laser processing like non-contact high-speed scribing. In order to avoid shunt formation across the edge of the laser scribe melting of the CIGS material during the laser irradiation has to be prevented [3, 4]. Due to the great challenge of laser scribing of the CIGS material without edge melting a great number of studies has been performed. In Ref. [5] various studies combining different laser parameters are summarized. In these studies it was found that even by using ultrashort laser pulses an edge melting cannot completely be avoided. In order to overcome these problems different new approaches have been reported. One approach for non-thermal laser structuring is SWIFD (shock wave-induced film delamination) [6]. At SWIFD the rear side of a substrate is irradiated with laser pulses which induce a partial ablation of the substrate and shock wave formation. The shock wave generates an interface stress at the front side of the substrate which can cause a delamination of the functional layer of the functional film at the substrate. The delamination effect of SWIFD is discussed in relation to thermally induced stress effects [7, 8]. It is shown that the SWIFD process can be used to scribe CIGS material with laser radiation without melting or thermally loading the CIGS material. Another approach for scribing of CIGS material is using thermomechanical processes in the interface between the CIGS and the substrate. The patterning of solar cells by removing the CIGS from the underlying Mo film can be achieved with nanosecond laser pulses at a wavelength of $\lambda = 1064$ nm but edge melting of the CIGS or damaging of the Mo film were observed regularly [5, 9, 10]. Due to the low absorption of the CIGS the NIR laser pulses can penetrate the CIGS film and can interact at the CIGS/Mo interface. Processes that might result are the partial evaporation of the Se at the CIGS/Mo interface [11] and stress formation at the interface [5]. The so-generated high interface stress causes a mechanical fraction and explosive flyaway of the CIGS material [11]. In the study of Lee et al. [5] the fracture of the CIGS film is explained by the partial absorption of the laser pulse energy at the surface of the CIGS film and the CIGS/Mo interface which causes an temperature difference between the front and rear side of the CIGS film. This temperature difference causes a thermomechanical stress in the CIGS film due to thermal expansion. By choosing the laser fluence in a range inducing a sufficient thermomechanical stress in the CIGS film, but lower than the melting temperature of the Mo film, the CIGS film can be removed without melting. The important process parameters used for this stress-assisted material removal process are the laser fluence and the optical properties of the CIGS film [5]. The band gap of the CIGS depends on the ratio of the composition elements whereas the relation between the band gap and the absorption coefficient for direct semiconductor materials is given by [12] $\alpha = A\sqrt{hf - E_g}$ with α absorption coefficient, h Planck constant, f frequency of light, E_g band gap energy, A constant. The band gap for commercial CIGS is adjusted by the Ga content. Typical Ga concentration values of 0% to 9% result in corresponding band gaps of $E_g = 1.03$ eV to $E_g = 1.23$ eV, respectively. [13] The photon energy at a laser wavelength of $\lambda = 1064$ nm (1.17 eV) is within this band gap range. Therefore, the composition ratio of the sample material is very critical, because slightly changes in the composition ratio influence the laser process drastically. To overcome this problem and stabilize the material removal process, laser sources with longer wavelengths are required in order to address the thermally induced stress effects to the CIGS/Mo interface instead to an ablation from the front side of the CIGS film. In the work of [14] it is shown that with laser sources having a wavelength of $\lambda = 1572$ nm and a pulse duration of 10 ps a delamination of the CIGS layer from the Mo layer is possible. Due to the high transparency of the CIGS and high absorption of the laser radiation at the CIGS/Mo interface the interface temperature rapidly rises, which triggers a localized spallation/lift-off process of the CIGS material [15, 16]. It could be shown that due to the lift-off process all the laser-effected CIGS material was mechanically removed from the Mo layer.

In the present study the results of laser scribing of CIGS with nanosecond laser pulses with a wavelength of $\lambda = 1550$ nm are presented. The results show that a removal of the CIGS layer from the Mo layer is possible without melting of the scribe edge or damaging of the Mo layer. It is also shown that the pulse overlap is a critical factor for a clean removal of the CIGS from the Mo. Scanning electron microscopy (SEM) imaging as well as energy-dispersive X-ray spectroscopy (EDX) was performed in order to analyse laser-induced modifications. In order to study the laser process more in detail micro-Raman analysis of laser scribed areas was performed. A penetration

depth for the λ = 532 nm laser wavelength was estimated in a 150–200 nm range for CIGS and in a 15–20 nm range for molybdenum layer, accordingly. Raman spectra were studied at 10 mW laser power and at room temperature.

2. Experimental set-up

For the experiments a laser source (LUSKENN from the Manlight company) providing a wavelength of λ = 1550 nm and a pulse duration of t = 6 ns was used. The maximum pulse energy of this laser source is up to E = 100 µJ and the tunable repetition rate up to f = 300 kHz. The laser source was embedded in a laser workstation (ILS 500x from INNOLAS SYSTEM). The laser beam with a nearly Gaussian intensity distribution was focused onto the sample surface by a scanner lens with a focal length of 100 mm. The laser spot size that was determined with the D^2 method has a diameter of d = 25 µm. The samples consisted of a 25 µm thick stainless steel sheet which was covered with a ~ 0.5 µm thick SiO_x thin film acting as an electrical isolator. On top of this SiO_x thin film a ~ 500 nm thick molybdenum layer and the CIGS film with a thickness of ~ 2 µm were deposited. A principle sketch of the sample material is shown in Fig. 1. After the laser scribing process the scribes were analysed by SEM in combination with EDX and optical microscopy (OM). In order to investigate possible material modifications Raman spectroscopy by using the confocal µ-Raman spectrometer/microscope (Thermo Scientific DXR) was applied. The Raman microscope has a 5.8 cm^{-1} resolution and was equipped with a 532 nm laser. Using an objective with 50 times magnification a laser spot size of up to 0.7 µm can be achieved.

Fig. 1. Sketch of the sample cross section used for the scribing experiments.

3. Results and discussion

In a first step the laser scribing of the samples was studied in systematic experiments with different laser fluences and scribing speeds. In Fig. 2 laser scribes are exemplarily shown which were generated with a fixed laser pulse energy of E = 18 µJ and a pulse repetition rate of 100 kHz. The scribing speed varied in a range between v = 10 mm/s and v = 3000 mm/s. In dependence on the scribing speed two different surface morphologies of the scribes could be distinguished. For low scribing speeds (see Fig. 2a) the edges of the scribes are melted and the bottom of the scribes is completely covered with melted material. Additionally, laser-induced periodic surface structures could be found in the bottom of the laser scribe. Deductive from the found surface morphology the dominant material process for low scribing speeds is ablation/evaporation, starting from the top side of the CIGS film. However, for high scribing speeds the surface morphology of the scribes (shown in Fig. 2c) is different from that for low scribing speeds. In particular, no sign of melting at the edges of the scribes could be found. Instead of that it seems that the CIGS film is fractured and removed as flakes from the samples. At the bottom of the scribe only the Mo surface seems melted. Comparing the optical microscope images of scribes, which were generated with low and high scribing speeds (Fig. 2 bottom), it can be seen that the bottom of the scribe is much more bright for the high scribing speed (see Fig. 2e) which indicates that with higher scribing speed the Mo film is almost completely cleared up from the CIGS film. This finding in combination with the found cracked edges of the scribe seen in Fig. 2 (left) indicates that the material removal process in the case of scribing with high scribing speeds is induced by mechanical stress near the interface between the CIGS and the Mo film. In Fig. 2b a laser scribe is shown which was generated with a moderate scribing speed. It can be seen in this SEM image that these features are caused by the

thermal and mechanical stress-dominated material processes. Partial melting and partial cracking of the edges of the laser scribe occur together. The two different scribing processes can also be distinguished by analysing the laser-generated scribes with optical microscopy imaging. In Fig. 2 (bottom) an optical microscope image of a laser scribe, which was generated with a high scribing speed (Fig. 2e), and an optical microscope image of a scribe, generated with a low scribing speed (Fig. 2a), are shown. In the image of the scribe generated with a high scribing speed the bottom of the scribe shows a much higher reflectivity than in the scribe which was generated with a low scribing speed. This difference in the reflectivity of the bottom of the laser scribes indicates also that in the case of laser scribing with low speeds material remains in the scribe or the Mo surface is modified, whereas the high reflectivity of high-speed scribes shows that the molybdenum is almost completely cleared up from the CIGS layer without surface modifications of the Mo.
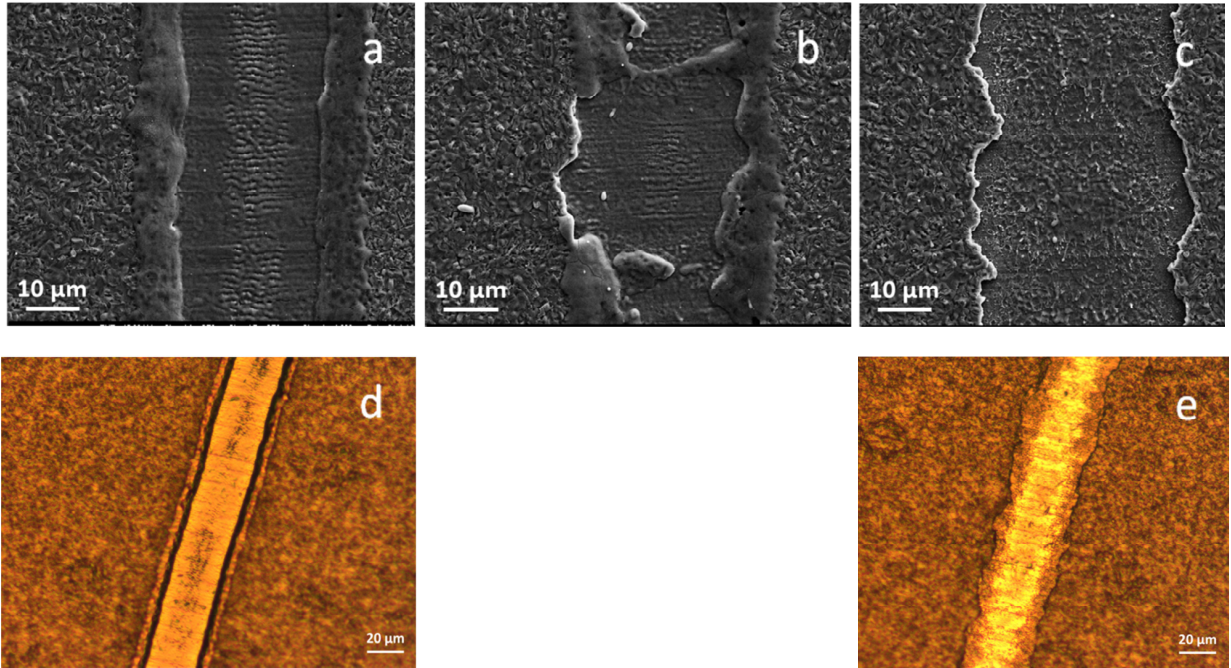

Fig. 2. SEM images (top) and optical microscope images (bottom) of laser scribes. The laser scribing used speed was v = 0.1 m/s; v = 0.3 m/s and 1.5 m/s, respectively. The laser pulse energy was fixed at a value of E_{Puls} = 18 µJ.

v [m/s]	E [μJ] 5.8	9	14	18	22	25	29	34	39	43	49
0.01	a	a	a	s	s	s	s	s	s	s	s
0.02	a	a	a	a	s	s	s	s	s	s	s
0.05	a	a	a	a	a	a	s	s	s	s	s
0.08	ü	a	a	a	a	a	a	a	s	s	s
0.1	ü	a	a	a	a	a	a	a	a	a	s
0.12	ü	a	a	a	a	a	a	a	a	a	a
0.15	ü	a	a	a	a	a	a	a	a	a	a
0.2	ü	ü	a	a	a	a	a	a	a	a	a
0.3	ü	ü	ü	ü	a	a	a	a	a	a	a
0.5	l	l	l	l	ü	ü	ü	ü	a	a	a
0.8	l	l	l	l	l	l	l	l	ü	ü	a
1	l	l	l	l	l	l	l	l	l	l	ü
1.5	l	l	l	l	l	l	l	l	l	l	l
2	l	l	l	l	l	l	l	l	l	l	l
2.5	n	l	l	l	l	l	l	l	l	l	l
3	n	l	l	l	l	l	l	l	l	l	l
5	n	n	n	n	l	l	l	l	l	l	l
10	n	n	n	n	n	n	n	n	n	n	n

Fig. 3. Summary of the CIGS scribing experiments (light green: ablation/melting; dark green: delamination/lift-off; yellow: transit region; red: full damaging Mo and/or stainless steel sheet; blue: single pulse).

In Fig. 3 the results of the analysis of the sample after the laser scribing process are colour-coded summarized (light green: melting, dark green lift-off, red: Mo layer damaged, blue: single pulses, yellow: transit region between melting and lift-off). In this Fig. 3 it can be seen that with increasing pulse energy the range of the transit between the thermal and mechanical stress-dominated material removal process decreases. By increasing the laser pulse energy from $E = 5.8\ \mu J$ to $E = 49\ \mu J$ the required scribing speed to enable a mechanical-like stress-induced CIGS material removal process increases from $v > 0.3$ m/s to $v > 1.0$ m/s. For a combination of very low scribing velocities and high laser pulse energies the Mo layer is ablated and the underlying stainless steel substrate is damaged. For very high scribing speeds $v > 5$ m/s the laser scribes are separated to single ablated dots. The energy range in which a mechanical stress-dominated material removal can be induced is in the investigated laser parameter field nearly independent from the laser pulse energy for a fixed scribing speed, respectively. This result is in contrast to previous studies which were performed with nanosecond laser pulses with a wavelength of $\lambda = 1064$ nm. In these studies, e.g. [5], is reported that the adjusting of the laser pulse energy is a critical factor to generate the mechanical stress-dominated material removal process.
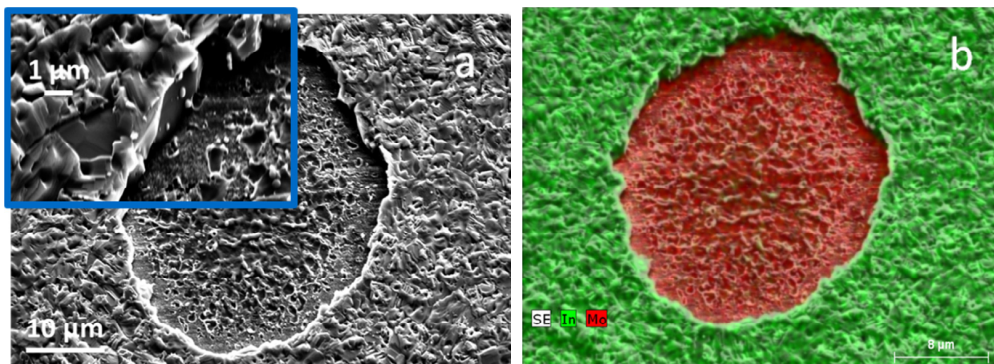

Fig. 4. SEM image (left) and EDX image (right) of an area which was irradiated with one single pulse ($E_{Pulse} = 18\ \mu J$). The inset shows a magnified section of the edge.

In Fig. 4 a SEM image of a single-pulse-irradiated area is shown. The inset shows a magnified section of the edge of the irradiated area. This image as well as the magnified inset shows no sign of melting of the edges. However, the exposed Mo layer seems modified due to the absorbed laser energy. In Fig. 4b the corresponding EDX image is shown. It can be seen that the CIGS film (represented in the EDX image by the Indium (In) signal) is nearly completely removed from the laser-irradiated area. Therefore, in this laser-irradiated area the Mo signal is clearly detectible. The melted material at the bottom of the laser-irradiated spot consists of Mo or a mixture of Mo and Se. In order to study the laser-induced modifications at the bottom of the laser scribes more in detail micro-Raman analysis were performed.

First the Raman spectrum of the non-modified CIGS layer (see Fig. 5) was characterized. A strong peak on 176 cm^{-1} can be assigned to the A_1 mode of CIGS.The second and third peaks were observed at 218 cm^{-1} and 250 cm^{-1} that can also be attributed to CIGS modes [17–19]. The position of the A_1 mode can vary due to the changeable Ga content in CIGS from 174 to 184 cm^{-1} (from CIS to CGS), as it is reported in Ref. [20]. The peak of the CIGS on 176 cm^{-1} shows that the sample contents a small amount of Ga. Due to the correlation of the Ga content the band gap energy is in the lower range of approximately $E_{gap} \sim 1.1$ eV [5, 13].
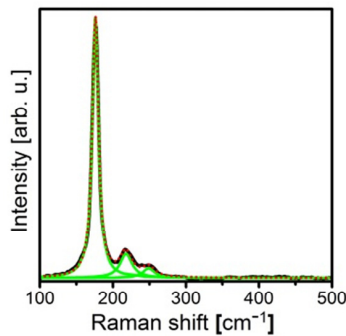

Fig. 5. Measured Raman spectra of an untreated area of the sample.

In a next step Raman spectra in laser-scribed areas were taken and analysed. After high-speed laser scribing these CIGS peaks were not detected By the low-speed process the peak intensity of the A_1 mode of CIGS was reduced by more than 91%. In Fig. 6 two Raman spectra after. scribing are shown. One was taken in the middle of a scribe which was generated with a high scribing speed (blue) (v = 1.5 m/s; E_{Pulse} = 18 µJ), the second Raman spectrum (green) was taken at a scribe which was generated with a low scribing speed (v = 0.1 m/s) but the same laser pulse energy. In this overview of the spectra it is seen that in both cases MoSe$_2$ is detectible, but in the spectrum taken from the low scribing speed a mixture of additional components, e.g. Se, CuGaSe$_2$ and CIGS, is found, which suggests that by scribing with high scribing speeds the undelaying Mo film is more cleared up then with low scribing speeds.
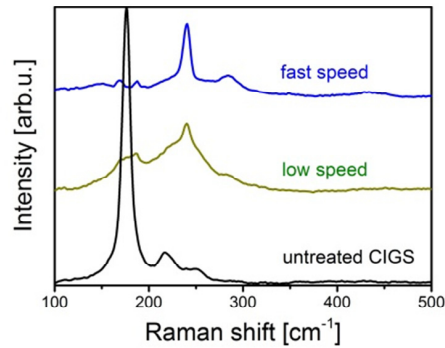
Fig. 6. Comparison of Raman spectra which were taken from areas which were scribed with high (v = 1.5 m/s; blue line) and low speed (v = 0.1 m/s, green line). The laser pulse energy was fixed at E_{Pulse} = 18 µJ for both scribes. For comparison the Raman spectra of an untreated area (black line) of the sample was added.

In Fig. 7 a detailed Raman spectrum of an area which was scribed with a low scribing speed is shown. The simplified reconstruction of this Raman spectrum allows localizing the important peaks. Components of $MoSe_2$ at 169 cm^{-1}, 240 cm^{-1}, 287 cm^{-1}, $CuGaSe_2$ at 187 cm^{-1}, $CuIn_xGa_{x-1}Se_2$ at 177 cm^{-1}, and Se at 235 cm^{-1} were observed. Peaks at 169 cm^{-1}, 240 cm^{-1}, and 287 cm^{-1} can correspond to E_{1g}, A_{1g} and E^1_{2g} modes of $MoSe_2$ [20-22], $CuGaSe_2$ has the strongest peak at 187 cm^{-1}. Two less intensive peaks of $CuGaSe_2$ are located at the same positions as the E_{1g} and A_{1g} modes of $MoSe_2$ [23].The broad peak at 235 cm^{-1} can correspond to trigonal selenium [24].

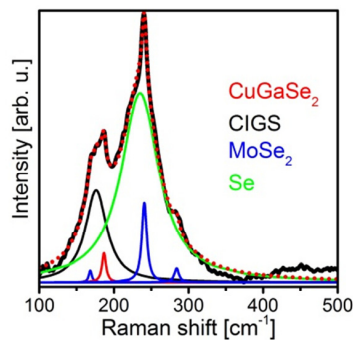Fig. 7. Raman spectra of an area which was scribed with a low scribing speed. (v = 0.1 m/s and E_P = 18 µJ). Colour code: blue: $MoSe_2$, black: CIGS, red: $CuGaSe_2$ and green: Se.

The next reconstructions of Raman spectra on processed area, generated with high scribing speed, are performed and shown in Fig. 8. The optical microscope image (see Fig. 8 top) of this scribe shows dark and light regions inside of the scribed area. In Fig. 8 (bottom) the Raman spectra taken in the dark (Fig. 8a) and light regions (Fig. 8b) are presented. In both spectra Se, $CuGaSe_2$, and $MoSe_2$ components with some additional new detected peaks were found. It can be assumed, that peaks at 108 cm^{-1}, and 150 cm^{-1} can be attributed to α- and γ-In_2Se_3 [25, 26]. The second-order scattering peak of $MoSe_2$ at 440 cm^{-1} was also observed. By comparison of the two spectra seen in Fig. 8 it can be assumed that in the dark region more Se content remains. The existence of MoO_3, MoO_2, SeO_2, and other oxide components were not detected in all analysed spectra. In **Fehler! Verweisquelle konnte nicht gefunden werden.** the peak position of the found structures are summarized.
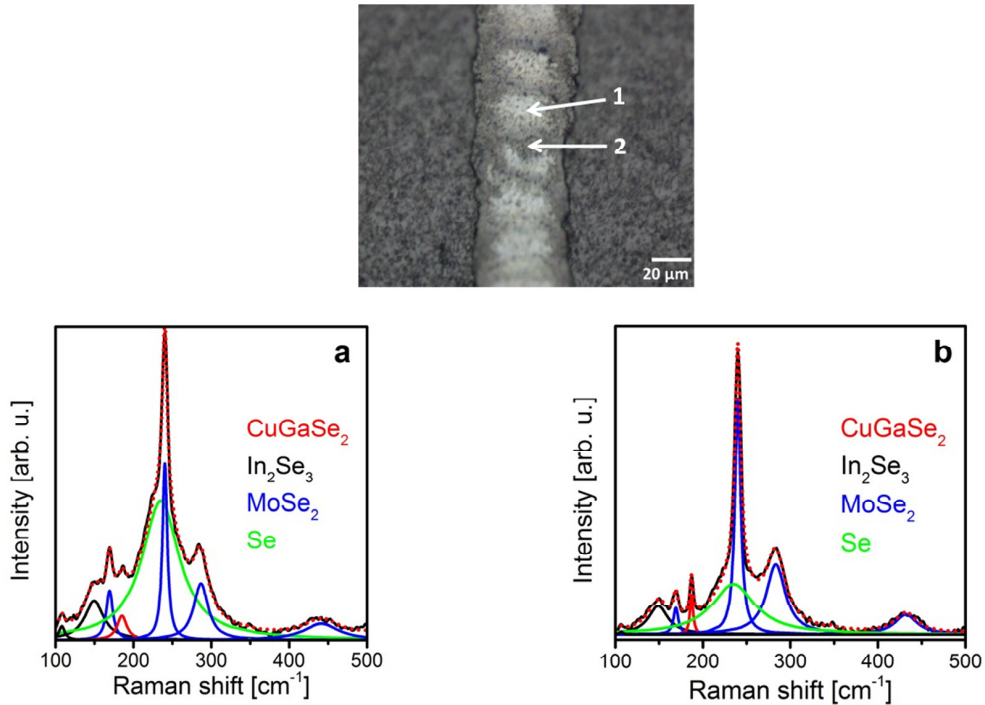
Fig. 8. (Top) Optical microscope image of a laser scribe which was generated with a high scribing speed. ($v = 1.5$ m/s and $E_{Pulse} = 18$ µJ). (Bottom) Raman spectra of laser scribes which were generated with a high scribing speed ($v = 1.5$ m/s and $E_{Pulse} = 18$ µJ). The spectra were obtained in the middle of the scribe on (a) dark region (marked in with "1") and (b) light region (marked with "2"). Colour code: blue: $MoSe_2$, black: In_2Se_3, red: $CuGaSe_2$ and green: Se.

Table 1. Peak positions of observed structures: Colour code: red: strong peak, blue: not observed.

Structure	CIGS	$MoSe_2$	$CuGaSe_2$	Se	α-In_2Se_3	γ-In_2Se_3
Peak position (cm^{-1})	176 218 250	169 240 287 350 440	169 187 199 240	235	108	150

4. Conclusion

In the present study the laser scribing of CIGS thin films on top of the Mo layer without edge melting or damaging the Mo layer is demonstrated. The scribing was performed with nanosecond laser pulses having a wavelength of $\lambda = 1550$ nm. A critical laser parameter to enable the mechanical removing of the CIGS without edge melting is the scribing speed. The scribing speed has to exceed a certain value to induce the delamination of the CIGS without edge melting and damaging of the Mo layer. The process window for inducing this effect was found to be broad in terms of scribing speed and laser pulse energy. The found results confirm that a damage-free scribing

of CIGS films is possible with nanosecond laser pulses having a wavelength of $\lambda = 1550$ nm, which gives the opportunity for using this nanosecond laser source, which is more efficient in terms of costs and stability.

Acknowledgements

References

[1] Cheyney, T., 2008. Thin-film CIGS starts to come of age. Photovoltaics International, 1, 86–92.

[2] press release Solar Frontier http://www.solar-frontier.com/eng/news/2015/C051171.html

[3] Wang, X., Ehrhardt, M., Lorenz, P., Scheit, C., Ragnow, S., Ni, X.W., Zimmer, K., 2014. The influence of the laser parameter on the electrical shunt resistance of scribed Cu(InGa)Se$_2$ solar cells by nested circular laser scribing technique. Applied Surface Science, 302, 194–197.

[4] Wehrmann, A., Puttnins, S., Hartmann, L., Ehrhardt, M., Lorenz, P., Zimmer, K., 2012. Analysis of laser scribes at CIGS thin-film solar cells by localized electrical and optical measurements. Optics and Laser Technology, 44, 1753–1757.

[5] Lee, S.H., Kim, C.K., In, J.H., Shim, H.S., Jeong, S.H., 2013. Selective removal of CuIn$_{1-x}$Ga$_x$Se$_2$ absorber layer with no edge melting using a nanosecond Nd : YAG laser. Journal of Physics D: Applied Physics, 46, (2013) 105502.

[6] Ehrhardt, M., Wehrmann, A., Lorenz, P., Zimmer, K., 2013. Patterning of CIGS thin films induced by rear-side laser ablation of polyimide carrier foil. Applied Physics A, 113, 309–313.

[7] Lorenz, P., Ehrhardt, M., Zimmer, K., 2014. Laser structuring of thin layers for flexible electronics by a shock wave-induced delamination process. Physics Procedia, 56, 1015–1023.

[8] Lorenz, P., Smausz, T., Csizmadia, T., Ehrhardt, M., Zimmer, K., Hopp, B., 2015. Shadowgraph studies of laser-assisted non-thermal structuring of thin layers on flexible substrates by shock-wave-induced delamination processes. Applied Surface Science, 336, 43–47.

[9] Buzas, A., Geretovszky, Z., 2012. Nanosecond laser-induced selective removal of the active layer of CuInGaSe$_2$ solar cells by stress-assisted ablation. Physical Review B, 85, 245304.

[10] Lee, S.H., Kim, C.K., In, J.H., Kim, D.S., Ham, H.J., Jeong, S.H., 2013. Nd:YAG laser ablation characteristics of thin CIGS solar cell films. Applied Physics B, 113, 403–409.

[11] Murison, R., Dunsky, C., Rekow, M., Dinkel, C., Pern, J., Mansfield, L., Panarello, T., Nikumb, S., 2010. CIGS P1, P2, and P3 laser scribing with an innovative fiber laser. Photovoltaic Specialists Conference (PVSC), 35th IEEE, 179–184.

[12] Rosencher, E., Vinter, B., *"Optoelectronics"*, 2002. Cambridge University Press, New York, pp. 744.

[13] Mudryi, A.V., Gremenok, V.F., Karotki, A.V., Zalesski, V.B., Yakushev, M.V., Luckert, F., Martin, R., 2010. Structural and optical properties of thin films of Cu(In,Ga)Se$_2$ semiconductor compounds. Journal of Applied Spectroscopy, 77, 371–377.

[14] Raciukaitis, G., Grubinskas, S., Gecys, P., Gedvilas, M., 2013. Selectiveness of laser processing due to energy coupling localization: case of thin film solar cell scribing. Applied Physics A, 112, 93–98.

[15] G. Račiukaitis, P. Gečys, S. Grubinskas, K. Zimmer, M. Ehrhardt, A. Wehrmann, A. Braun, 2012. Laser Structuring of Thin Films for Flexible CIGS Solar Cells, Photovoltaics International, 17, 91-98.

[16] Gečys P., Markauskas E., Dudutis J., Račiukaitis G., 2014. Interaction of ultra-short laser pulses with CIGS and CZTSe thin films, Applied Physics A, 114, 231-241

[17] Wang J., Qiao Y., Zhu J., 2015, Microstructure characterization of the soda-lime-glass/copper–indium–gallium–selenium interface in Cu-poor Cu(In,Ga)Se2 thin films, Thin Solid Films, 583, 50-54.

[18] Han J., Ouyang L., Zhuang D., Liao C., Liu J., Zhao M., Cha LM., Besland MP., 2014, Raman and XPS studies of CIGS/Mo interfaces under various annealing temperatures, Materials Letters, 136, 278-281.

[19] Li M., Zheng M., Zhou T., Li C., Ma L., Shen W., 2012, Fabrication and centeracterization of ordered CuIn(1−x)Ga x Se2 nanopore films via template-based electrodeposition, Nanoscale Research Letters, 7, 1-6.

[20] Witte W., Kniese R., Eicke A., Powalla M., 2006, Influence of the GA Content on the Mo/Cu(In,Ga)Se2 Interface Formation, IEEE 4th World Conference on Photovoltaic Energy Conference, Waikoloa, HI, 2006, pp. 553-556.

[21] Nam D., Lee JU, Cheong H, 2015, Excitation energy dependent Raman spectrum of MoSe2., Scientific Reports 5: 6

[22] Sekine T., Izumi M., Nakashizu T., Uchinokura K., Matsuura E., 1980, Raman Scattering and Infrared Reflectance in 2H-MoSe2., J. Phys. Soc. Jpn. 49, pp. 1069-1077

[23] Rincon C., Ramirez FJ., 1992, Lattice vibrations of CuInSe2 and CuGaSe2 by Raman microspectrometry, J. Appl. Phys., 72, 4321-4324.

[24] Nagels P., Sleeckx E., Callaerts R., 1995, L. Tichy, Structural and optical properties of amorphous selenium prepared by plasma-enhanced CVD, Solid State Communications, 94, 49-52.

[25] Weszka J., Daniel P., Burian A., Burian AM., Nguyen AT., 2000, Raman scattering in In2Se3 and InSe2 amorphous films, Journal of Non-Crystalline Solids, 265, 98-104.

[26] Kambas K., Julien C., Jouanne M., Likforman A., Guittard M., 1984, Raman Spectra of α- and γ-In2Se3, physica status solidi (b), 124, 105-108.